SNO-STR-91-047

Producing Čerenkov Photons From Low Energy Electrons With EGS4

M. D. Lay, D.L. Wark
R.J. Boardman

Nuclear Physics Laboratory,
University of Oxford,
Keble Road, Oxford
OX1 3RH

June 18, 1991

1 Introduction.

All of the Monte Carlo codes currently available for SNO use EGS4 to propagate the electrons and gammas created by neutrino interactions. It is therefore important to demonstrate that the EGS4 code performs this task correctly, specifically that EGS4 (as modified by the collaboration to produce Čerenkov radiation) produces the proper number and angular distribution of Čerenkov photons for an electron or gamma of a given energy. However, very little work has been done on EGS4 at low energies (see Rogers [2]), so the purpose of this report is to compare EGS4 predictions against experimental data in order to see how accurate the code is at low energies (low in this case means less than $\sim$ 20 MeV but greater than the Čerenkov threshold), and, where necessary, suggest solutions to any problems discovered.

Apart from the user specified parameters, such as the material of interest and the initial energy of the particle etc, EGS4 relies on three external parameters - AE, AP and ESTEPE [3].

AE is the energy below which the program will no longer track an electron individually.

Knock on electrons will not be produced if their energy would be below this energy - instead this energy loss is factored into the continuous energy loss. Technically, the value of AE includes the rest mass of the electron, but, in order to conform to the way other energies are quoted, this paper will list only the kinetic energy part of AE.

AP works in a similar way for the photons. This parameter was not found to be a problem in any of this work, and will not be specifically referenced in later sections.

ESTEPE is a constraint on the maximum energy loss in any one step that the program will allow. If ESTEPE is not specified, or is set to 0%, the default maximum energy loss depends on several variables (including the geometric constraints, the probability of a discrete interaction, AE, AP). This default was designed to get agreement with data at high energies, and at high energies leads to very small energy losses per step. However, this is not the case for low energies (about 20 MeV or less), where the maximum energy loss per step can rise to around 25%. This introduces inaccuracies because the program is then sampling various quantities, such as the stopping power and the multiple scattering angle (both of which are energy dependant), at large energy differences. The subroutine FIXTMX is used to set this limiting factor so that the electron cannot lose more than a fixed fraction of it's energy (ESTEPE) via continuous energy loss in any one step. This is explained more thoroughly by Rogers [2]. It should also be noted that the value of ESTEPE has a lower bound - if the maximum step length is too short then multiple scattering starts to become 'switched off'. This lower limit is dependant on the material, and drops with increasing Z. This is more fully discussed by the EGS4 authors [3].

These parameters not only effect the results of the Monte Carlo, they also effect the running time of a particular problem quite dramatically. The effect of setting ESTEPE to 1% instead of the default is to increase the running time by a factor of approximately 25. The running time of any simulation also increases as AE (or AP) is reduced. This is obviously because the number of particles to be tracked increases as the minimum energy a particle must have, in order to be tracked individually, decreases. For example, with electrons stopping in perspex the difference in running with AE set at 51 keV and set at 1 MeV is a factor of 10 in the running time. Thus, unless there are good reasons not to do so, the obvious choice would be to run the program with ESTEPE set at the default, and a high value of AE. Unfortunately, this does not always produce correct results.

2 Stopping Powers.

The stopping powers for perspex and water have been calculated using the EGS4 code system for energies ranging between 0.4 MeV and 20 MeV, and compared with the ICRU table of stopping powers [5]. These two materials were chosen because of their use in the SNO detector.

The EGS4 code system makes a distinction between continuous and discrete energy loss. The former consists of interactions that would result in a particle being created with an energy less than the cutoff energy, together with the energy loss due to the emission of Bremsstrahlung radiation. The latter case corresponds to the creation of secondary particles (with energies greater than the cutoff energy), which carry off some proportion of the original particle's energy, and are tracked independently. The sum of these two is the total energy loss, and this should not depend on the value of the cutoff energy. Varying the cutoff energy in the range 50 keV to 1 MeV produced no noticeable effect on the calculated stopping powers, except to change the minimum energy of the calculation. This suggests that there are no errors in the way the code aportions the continuous and discrete energy losses (at least for the range 50

keV to 1 MeV). If there was an error, the stopping powers should have altered as the value of the cutoff energy was varied, because this marks the boundary between continuous energy loss and discrete energy loss.

The EGS4 predictions agree well with the ICRU tables (see figures 1 and 2), and dividing the predicted values of the stopping power by the ICRU data gives an average ratio of 0.996 ± 0.010 for perspex and a ratio of 0.994 ± 0.012 for water. Changing ESTEPE produces no noticeable change in the calculated values of the stopping power; dividing the predicted stopping power with ESTEPE at 1% by the stopping powers predicted with ESTEPE set at 5% gives 1.000 ± 0.018, whilst comparing the default (ESTEPE $\sim$ 25%) with the 1% predictions gives 1.000 ± 0.019

These simulations show that the calculation of stopping powers is very insensitive to the value of ESTEPE used.

3 Multiple Scattering Of Electrons

The multiple scattering of electrons in thin foils has been calculated and compared with experiment. In all cases it is assumed that the electron beam is monoenergetic, and that it strikes the foil normally.

As a charged particle traverses a medium, it may be deflected by many small angle scattering events. These events are mostly due to coulomb scattering from the nucleii and atomic electrons, and multiple scattering is well described by the theory of Molière [11], [12]. For small deflection angles the angular distribution of multiply scattered particles is approximately Gaussian, and, using this approximation, the width θ_0 of the angular distribution has been found [8] to be

$$\theta_0 = \sqrt{2}\,\frac{13.6\ MeV}{\beta cp} z \sqrt{\frac{x}{X_0}} \left[1 + 0.038 \ln\left(\frac{x}{X_0}\right)\right] \tag{1}$$

where βc, p, and z are the velocity, momentum (MeV/c) and charge number of the incident particle, and x/X_0 is the ratio of sample thickness to the radiation length for that material. For all the targets used by Kulchitsky and Latyshev [10], $x/X_0 \approx 10^{-2}$, so the formula simplifies to

$$\theta_0 \simeq \frac{constant}{\beta cp} z \sqrt{\frac{x}{X_0}} \tag{2}$$

The radiation length can be approximated [8] to be

$$X_0 \simeq \frac{716.4\ g\ cm^{-2}\ A}{Z(Z+1) ln(287/\sqrt{Z})} \tag{3}$$

Thus, to a rough approximation, the width of the angular distribution of the multiply scattered electrons will be proportional to $Z\sqrt{x/A}$.

A more detailed analysis [9] leads to the relation

$$\theta_0 = \chi_c \sqrt{B - 1.2} \tag{4}$$

where

$$\chi_c^2 = 4\pi N\ Z(Z+1) e^4/(p\beta c)^2 \tag{5}$$

$$\chi_a^2 = (\hbar Z^{1/3}/0.885 p a_0)^2 [1.13 + 3.76(Z/137\beta)^2] \tag{6}$$

$$\Omega_b = 7e^B/6B = \chi_c^2/\chi_a^2 \tag{7}$$

where N is the number of atoms/cm^2 and a_0 is the Bohr radius. Equation 7 may be solved numerically.

The information from the Monte Carlo was analysed by histogramming the data and then fitting to a skewed gaussian, assuming $\sqrt{n}$ errors in the data. The width (defined as the point at which the function fell to $1/e$ of its value at 0°) of the skewed gaussian was then calculated. This procedure is necessary to avoid what appears to be a problem with the EGS4 code. Figures 3 and 4 show the angular distribution of the electrons for one particular run. As can be seen, the raw data (binned as fractional scattering at an angle) shows a 'plateau' structure, which, when divided by $\sin\theta$ (in order to get the fractional scattering per square degree), appear as a series of peaks. This only appears when the angular distribution is scrutinised too closely - if the graph in figure 4 were rebinned with 4 bins in 1, the structure would mostly wash out (see figure 5). However, there would still be problems close to $\theta = 0$, which is unfortunate, considering the definition of the width. Hence the fitting procedure used. It is speculated that the problem arises from the way the code converts a probability function into an angular function, though this has yet to be confirmed.

Kulchitsky and Latyshev [10] have measured the multiple scattering of monoenergetic electrons at 2.25 MeV for a wide variety of elements, ranging from Aluminium (Z=13) to Lead (Z=82), and have listed the width of the angular distribution for them. However the results presented for tin and gold seem to contradict the other results, as well as being in wild disagreement with both the Molière theory predictions and the Monte Carlo calculation. For example, a thin foil of gold should scatter the electrons more than a similar sized foil of tantalum, as it has a higher Z value, and a higher density, whereas the quoted scattering widths are 9.20° for gold and 9.85° for tantalum. Using the formulae above, it can be shown that the results for gold and tin contradict the other results and hence the results for these two elements have not been used. The experimental results for the other seven elements agree well with the predictions of Molière theory, though there is a slight problem with the theoretical predictions in that they rely on p the momentum of the particle, and, as the electrons lose a non negligible fraction of their energy in the foil, this is not a constant. Thus there is an added uncertainty introduced into the calculated Molière width due to averaging over the momentum. The data can be found in table 1. In all cases, the width predicted by EGS4 was found to be notably less than either the experimental values or the value predicted by Molière theory.

Changing ESTEPE (from the default through to 1%) has no statistically significant effect on the width predicted by the Monte Carlo. The exception to this was aluminium, in which the predicted width for ESTEPE at 1% is $\sim 0.15°$ less than the width with ESTEPE at the default. This is an example of the multiple scattering being 'switched off' - see the earlier discussion on the EGS4 code system. When this happens, there is less scattering, and hence the width is narrower. Performing the calculations with ESTEPE at 3% restores the agreement with the value predicted by the default setting of ESTEPE.

Changing the value of AE in the range 5 keV to 1 MeV causes a slight increase in the angle with the decrease in AE. This is due to the fact that electrons which are scattered into large angles are more likely to be 'cut' as their energy drops below the cutoff energy before they can exit the material. This cutting of electrons that suffer large angle scattering will tend to narrow the width of the remaining distribution.

Hanson et al [9] have measured the multiple scattering of 15.7 MeV electrons by thin gold and beryllium foils. They list two approximations to the width of the distribution, both of which are given in table 2, along with the experimental and Monte Carlo data. In this case the Monte Carlo predictions agree well with the Molière predictions, though both have a tendency to overestimate the width, compared with the experiment. Even so the disagreement is only

of the order of 5%. Changing ESTEPE has no observable effect on the width. Reducing AE has the effect of slightly widening the distribution via the mechanism discussed above.

The conclusion of this section is that EGS4 underestimates the width of the distribution at low energies by approximately 4% on average. This disagreement tends to increase with increasing Z. Altering the values of the cutoff energy and ESTEPE have no noticeable effect on the width, unless the value of ESTEPE is so low as to start to switch off the multiple scattering. At higher energies, the agreement between the experimental data and the Monte Carlo predictions is much better, though in this case the program tends to overestimate the width of the distribution; either of the value of the cutoff energy or ESTEPE still have little effect on the predicted width. Again, the width for gold is relatively narrower than the width for beryllium, suggesting that there is some form of Z-dependency in the multiple scattering formalism that is not quite correct. The multiple scattering of electrons from the nucleus is proportional to Z^2, but to take into account the scattering from the atomic electrons, the data preparation package, PEGS, adjusts this to Z(Z+$FUDGEMS), where the default value of $FUDGEMS is 1 - see Rogers [2].

4 The Backscattering Coefficient Of Electrons.

There is an extensive body of data on the backscattering coefficient of electrons for a variety of elements in the literature, and this is well reviewed by Tabata et al [13]. They have suggested an empirical equation for the backscattering coefficient η of the form

$$\eta = \frac{a_1}{(1 + a_2 \tau^{a_3})} \tag{8}$$

where τ is the incident kinetic energy in units of the rest energy of the electron, and a_1, a_2 and a_3 are constants for each element. They may be determined by experiment, or derived from the following equations -

$$a_1 = b_1 \exp(-b_2 Z^{-b_3}) \tag{9}$$

$$a_2 = b_4 + b_5 Z^{-b_6} \tag{10}$$

$$a_3 = b_7 - b_8/Z \tag{11}$$

where b_i are constants, independent of Z. These constants are listed in Tabata's paper.

Experimentally, η is defined as the total number of electrons detected in the back hemisphere, divided by the total number of electrons incident on the target. A small voltage (usually of the order of 100 volts) is applied between the detector and the sample, in order to filter out low energy secondary electrons, though high energy secondary electrons will still be counted as backscattered. However, this voltage is too low to simulate by setting the cutoff energy to the equivalent energy, because the processing time would be unfeasibly long, so the effect of a higher value of AE must be examined. Although many low energy secondary electrons may be created, their range is correspondingly small, so the chances of these electrons adding to the backscattering coefficient must be modified by the chances of these electrons being created near enough to the back of the target to escape and be detected.

For aluminium, at low energies, and with ESTEPE set to 3%, the cutoff energy does not appear to present too much of a problem. The percentage of backscattered electrons lost below the cutoff was estimated by generating the kinetic energy spectrum of backscattered electrons for these energies with cutoff energies of 50, 100 and 150 keV. A skewed gaussian was fitted through the low energy part of the spectrum, and the number of 'missing' electrons in the first three 50 keV bins was estimated. The estimated numbers of missing electrons for all

three cutoffs (at any particular energy of incident electron) agreed to within statistical errors. Secondly, the number of missing electrons was estimated by averaging over the accessible bins in each spectra (the 50 - 100 keV and 100 - 150 keV bins for the 50 keV cutoff, and the 100 - 150 keV bins for the 100 keV cutoff). This gave results in agreement with the first method. At 1 - 2 MeV, the fraction of backscattered electrons lost because of the cutoff is estimated to be 2% of the total number of backscattered electrons per 50 keV of AE up to 150 keV. At 5 MeV, this percentage rises to approximately 3.5%, and at 10 MeV the percentage is 6.5%. This rise appears to be approximately linear, provided that the value of AE is small compared with the initial energy of the incident electron. Changing ESTEPE to the default increases the deficit of electrons by a further 2% (on average) at all energies. For carbon, the deficit is estimated to be 4.5% at 1 MeV, 4.0% at 2 MeV, 7.1% at 5 MeV and 8.5% at 10 MeV. However the statistics are poor, and the uncertainty in these percentages is of the order of 1/4 of their size. For gold the percentage of backscattered electrons lost in this way is approximately constant at 0.9% (per 50 keV of the cutoff) in the range 1 to 10 MeV.

Having established the effect of AE, what is the effect of ESTEPE? As can be seen from figure 6 (which shows the predicted backscattering coefficient from aluminium, with AE set at 51 keV), the default value, which appears to be equivalent to ESTEPE of 20-25%, underestimates the backscattering coefficient for all energies, by an amount that is not explicable by the cutoff energy correction discussed above. The predicted backscattering coefficient depends strongly on the value of ESTEPE, and a value of 3% gives the best fit to the data, in the energy range of 1 to 12 MeV. There is little data for backscattering from silicon at energies of more than 1 MeV, but what data is available ([14], [15]) agrees well with the predictions made using Tabata's equations (9 - 11), and these predictions were extrapolated to higher energies using equation 8 (see figure 7). Accounting for the error induced by the cutoff energy, ESTEPE = 3% was again found to give the best fit to the data (see figure 8). The data for carbon seems to be much poorer (Tabata et al reported a relative rms deviation from their best fit line of 23%, compared with 8.3% for aluminium), and there seems to be a considerable amount of disagreement in the data, especially for incident energies of approximately 1 MeV - see figure 1a in Tabata et al. This is presumably due to the very low backscattering coefficient ($\sim$ 1.6% at 1 MeV), and the effect that has on the statistics. In this case the best agreement with the data was found to be with ESTEPE at 6% (figure 9).

For higher Z elements, the EGS4 predictions show a significant deviation from the data (see figure 10), and no explanation has been found for this. It has been noted that reducing ESTEPE increases the predicted backscattering coefficient (figure 11), but it has not been possible to reproduce the reported backscattering coefficients, in a reasonable amount of processing time.

A study of the kinetic energy spectra of the backscattered electrons was also found to be of interest, and such data may be found in the paper by Rester and Derrickson [16] for aluminium, iron, tin and gold with incident electrons of 1 MeV. The graph in figure 12 illustrates some interesting points. As can be seen, the predictions for the kinetic energy spectrum agree well with the experiment, but the prediction appears to have two cutoffs. The low energy cutoff is obviously due to AE; as no electrons with an energy less than AE are propagated, no electrons will be found to be backscattered with such an energy. The high energy cutoff corresponds to an energy loss of twice ESTEPE, and represents an electron taking one maximum length step into the material, being scattered, and coming straight out again. Very rarely events are produced with energies above this limit, corresponding to electrons that do not take a full step into the medium before suffering a large angle scatter.

The conclusion of this section is that the predictions for the backscattering coefficient are not strongly dependent on AE, and, given that the Čerenkov threshold (discussed later)

will eliminate any effect of the cutoff energy, no 'optimum value' is suggested. The predicted coefficient is strongly dependant on the value of ESTEPE, and for the purposes of the SNO experiment, a value of 3% is recommended, based on the results obtained for aluminium and silicon. The results for carbon suggest a value of 6% would be more appropriate, however, the experimental data is often contradictory, and these results have been given less weight in determining the best value of ESTEPE.

5 Čerenkov Radiation Production.

The amount of Čerenkov radiation can be calculated from the theory of Frank and Tamm [6], see Jelley [4], which predicts the yield of N Čerenkov photons per unit angular frequency $d\omega$, per unit track length dx, from an electron of velocity βc, as

$$\frac{d^2N}{d\omega\, dx} = \frac{\alpha}{c}\left(1 - \frac{1}{\beta^2 n^2}\right) \qquad \text{when} \qquad \beta^2 n^2 \geq 1\,, \tag{12}$$

where n is the refractive index and α is the fine structure constant.

Integrated over the electron's path, this becomes

$$\frac{dN}{d\omega} = \int_{path\ length} \frac{\alpha}{c}\left(1 - \frac{1}{\beta^2 n^2}\right) dx \tag{13}$$

which can be calculated by numerically integrating along each electron's path.

The EGS4 code can be used to calculate the total amount of Čerenkov radiation produced by the initial electron and its associated secondary electrons, but can also be set to give the amount of Čerenkov radiation produced by the initial electron only (ignoring the contributions from any secondary electrons produced). The number of Čerenkov photons produced per unit frequency has also been calculated using a direct integral method, which assumes the theory of Frank and Tamm, as well as the tabulated stopping powers [5]. The electrons are assumed to be stopping in an isotropic perspex block, which has a density of 1.182 g/cm^3 and a refractive index of 1.5.

The data from the two calculations agree well at the lower energies, but at energies higher than a few MeV, the direct integration method produces significantly less light than the EGS4 calculation. This can be accounted for by remembering that the direct integration takes no account of the contribution to the Čerenkov radiation from any secondary electrons (δ-rays) that might be produced. At low energies, this contribution is negligible, but the proportion of Čerenkov radiation produced by secondaries increases with the energy of the initial electron. Plotting the data from the direct integration against the EGS4 predictions for the amount of light produced by the initial electron only restores good agreement. For more details of the direct integration method see 'Low Intensity Sources Of Čerenkov Radiation' [7].

As can be seen from table 4, the amount of Čerenkov radiation produced has little dependance on the value of AE, provided that AE is below the threshold for the production of Čerenkov radiation (about 175 keV for perspex). There is a slight dependance on the value of ESTEPE (table 3), with the amount of Čerenkov radiation produced rising as the value of ESTEPE rises. The default version of the code was found to produce approximately 2% more Čerenkov radiation than when ESTEPE was set at 1%. This can be understood by considering that at small values of ESTEPE, the program is sampling the electron's energy at many points throughout it's path, and thus is properly averaging over the path, whereas with a high value of ESTEPE, the program will tend to sample the electron's energy at wider gaps, and furthermore will tend to get a slightly higher average.

It should be noted that, as the amount of Čerenkov radiation produced is dependant on the stopping power of the medium, this relative insensitivity to the parameterisation of AE and ESTEPE cross-references well with the calculations for stopping powers, which were also insensitive to these parameters.

6 The Directional Production Of Čerenkov Radiation.

One of the important considerations in the SNO detector is the ratio of Čerenkov light in the backward and forward hemispheres, where the 'backward hemisphere' is defined with respect to the initial direction of the incident electron. This ratio has an effect on how accurately the interaction vertex can be located; the more light in the backward hemisphere, the better the vertex resolution. However, previous sections have shown that

1. the backscattering coefficient is strongly dependant on the value of ESTEPE. The dependance on the cutoff energy can be ignored for this application, as low energy electrons will not produce Čerenkov radiation.

2. the calculated stopping powers are independent of either ESTEPE or the cutoff energy.

3. the amount of Čerenkov radiation produced is largely independent of ESTEPE and the cutoff energy.

The third point is encouraging because it indicates that the parameters AE and ESTEPE can be optimized on the basis of experimental data without effecting this. However the first two points suggest that the angular distribution of electrons that are scattered through large angles is dependant on the value of ESTEPE, and thus the angular distribution of Čerenkov radiation would also be expected to be dependant on ESTEPE.

The theory of Frank and Tamm [6] shows that the Čerenkov radiation will be emitted in a cone whose opening angle with respect to the particle's direction of travel is given by

$$\theta_c = \cos^{-1}(1/\beta n) \tag{14}$$

Figure 13 shows the ratio of backwards to forwards Čerenkov radiation for ESTEPE at the default, and with ESTEPE set at 3%. As can be seen, the default underestimates the ratio, compared with the ESTEPE = 3% prediction by an amount between 25% and 75%. The ratio is roughly constant in the range for ESTEPE of 1-6%, but drops off rapidly after that. Thus, although it would appear that using the default gives the wrong answer, there is considerable room for choosing an appropriate value of ESTEPE. The results for the backscattering coefficient of carbon, aluminium and silicon suggest that the correct value for ESTEPE is somewhere in the range 3-6%. The value of AE has no effect on the calculation, provided that it is below the threshold for the Čerenkov radiation production.

7 Application to the SNO Monte Carlo.

The information derived above has been applied to the existing SNO Monte Carlo programs with the following results:

1. The Queen's code does not have a version of FIXTMX linked to it, instead, the program uses a routine whereby the maximum step length is limited to 0.01 radiation lengths for electrons with energies of greater than 5 MeV, and to 0.001 radiation lengths for electrons with less than that energy. This seems to quantitatively reproduce the correct forward/backward

ratio of Čerenkov radiation photons at the $\sim$ 1% level (see table 5) with a factor of two increase in speed over EGS4 with ESTEPE set at 3%.

There is a slight bug with the Queen's code, however, when one compares the absolute numbers of photons produced. This seems to come from the routine which does a crude numerical integration to determine the area under the curve of the quantum efficiency as a function of wavelength. For example, when a quantum efficiency function with only 8 points was used, the Queen's code predicted 20% more Čerenkov photons compared to the work described above. When the function was represented by 71 points, this discrepancy was reduced to less than 3%. We are therefore putting a proper numerical integration routine into the code and will distribute it when debugged.

2. As far as we can tell the UCI code uses EGS4 with the default value of ESTEPE. It will therefore underestimate the production of photons in the backward hemisphere (see figure 13). This may help to explain some of the differences in results between the two codes, as these backward photons are very helpful in fitting the vertex. This can be corrected by using ESTEPE = 3%, however the fix used in the Queen's code seems to produce the same result with a considerable savings in running time.

References

[1] G Aardsma *et al*, (1987), Phys Lett B **194**, 321.

[2] DWO Rogers Nucl. Instr. Meth., **227**, 535-548 *Low Energy Transport With EGS*

[3] Walter R Nelson, Hideo Hirayama and David WO Rogers, (1985) *The EGS4 code system*, SLAC report 265.

[4] JV Jelley, (1958) *Čerenkov Radiation*, Pergamon Press, London.

[5] ICRU (1984). International Commission on Radiation Units and Measurements. *Stopping Powers for Electrons and Positrons*, ICRU Report 37 (International Commission on Radiation Units and Measurements, Bethesda, Md. 20814 USA).

[6] IM Frank and Ig. Tamm, (1937) *Dokl. Akad. Nauk, SSSR*, **14** (3), 109.

[7] RJ Boardman, MD Lay, NW Tanner and DL Wark, (1991). *Low Intensity Sources Of Čerenkov Radiation.* To appear as a SNO publication.

[8] Particle Data Group (1990) Phys. Let. B **239**

[9] AO Hanson, LH Lanzl, EM Lyman, MB Scott (1951) Phys. Rev. **84** 634. *Measurement of Multiple Scattering of 15.7-MeV Electrons*

[10] LA Kulchitsky and GD Latyshev (1942) Phys. Rev. **61** 254.

[11] G Molière Z. Naturforsch 3a, 78 (1948); 2a 133 (1947)

[12] HA Bethe (1953), Phys. Rev. **89**, 1256

[13] T Tabata, R Ito and S Okabe (1971) Nucl. Instr. Meth. **94** 509-513. *An Empirical Equation For The Backscattering Coefficient Of Electrons*

[14] DH Rester and WJ Rainwater Jr (1966) Nucl. Instr. Meth. **41** 51-55 *Backscattering of 1-MeV Electrons From Silicon*

[15] A Damkjaer (1982) Nucl. Instr. Meth. **200** 377-381 *The Response Of A Silicon Surface Barrier Detector To Monoenergetic Electrons In The Range 100-600 keV.*

[16] DH Rester and JH Derrickson (1970) Nucl. Instr. Meth. **86** 261-267 *Electron Backscatter Measurements For Perpendicular and Non-Perpendicular Incidence At 1 MeV Bombarding Energy.*

8 The Tables.

Element	Width (Experiment)	Width (Molière Theory)	EGS4 Predictions AE=1 MeV ‖ AE=500 keV ‖ AE=51 keV .....ESTEPE.....					
			0.00	0.01	0.00	0.01	0.00	0.01
Aluminium	9.50	9.76	9.17	9.17	9.18	9.03	9.25	9.09
Iron	9.60	9.68	9.20	9.22	9.20	9.25	9.33	9.31
Copper	10.40	10.76	10.11	10.09	10.04	10.03	10.24	10.25
Molybdenum	10.25	10.29	9.64	9.64	9.71	9.73	9.68	9.69
Silver	10.20	10.30	9.70	9.69	9.71	9.71	9.72	9.80
Tantalum	9.85	10.10	9.45	9.45	9.50	9.51	9.49	9.50
Lead	9.70	9.71	9.06	9.06	9.09	9.09	9.11	9.11

Table 1: Comparison of the EGS4 Predictions against the data of Kulchitsky and Latyshev. Statistical errors in the monte carlo predictions are ± 0.04°. All angles in degrees.

Element	Sample Thickness (mg/cm^2)	Width (Experiment)	Width (Molière Theory)	EGS4 Predictions AE=1 MeV ‖ AE=51 keV .....ESTEPE.....				
				0.00	0.01	0.05	0.00	0.01
Beryllium	257	3.06	3.13/3.16	3.16	3.12	3.16	3.24	3.17
Beryllium	495	4.25	4.57/4.63	4.54	4.56	4.54	4.69	4.67
Gold	18.66	2.58	2.52/2.81	2.57	2.58	2.57	2.60	2.60
Gold	37.28	3.76	3.83/4.21	3.88	3.88	3.88	3.90	3.91

Table 2: Comparison of the EGS4 Predictions against the data of Hanson et al. The two Molière predictions given arise from two approximations given by Hanson et al. Statistical uncertainties in the monte carlo predictions are ± 0.02°. All angles are given in degrees.

ENERGY	2 MeV		5 MeV		10 MeV		20 MeV	
ESTEPE	Total	Primary	Total	Primary	Total	Primary	Total	Primary
0.01	0.95	0.94	2.84	2.76	5.96	5.59	12.02	10.70
0.02	0.95	0.94	2.87	2.79	6.04	5.65	12.06	10.79
0.05	0.96	0.95	2.86	2.76	5.99	5.62	12.07	10.76
default	1.00	0.99	2.91	2.81	6.05	5.66	12.23	10.92

Table 3: The Production of Čerenkov radiation . $\frac{dN}{d\omega} \times 10^{-13}$ against energy. 'Total' refers to the total amount of Čerenkov radiation produced, 'Primary' refers only to the Čerenkov radiation produced by the primary electron only, mimicking the classical calculation.

ENERGY	2 MeV		5 MeV		10 MeV		20 MeV	
AE	Total	Primary	Total	Primary	Total	Primary	Total	Primary
51	0.95	0.94	2.85	2.76	5.98	5.63	12.09	10.83
150	0.95	0.94	2.84	2.75	5.97	5.60	12.05	10.75
1000	0.59	0.59	2.41	2.39	5.37	5.20	11.11	10.34

Table 4: The Variation of the production of Čerenkov radiation with AE. $\frac{dN}{d\omega} \times 10^{-13}$ against energy. 'Total' refers to the total amount of Čerenkov radiation produced, 'Primary' refers only to the Čerenkov radiation produced by the primary electron only, mimicking the classical calculation.

ENERGY	> 90°		> 120°		> 150°	
(MeV)	Queen's	EGS4	Queen's	EGS4	Queen's	EGS4
2.0	11.4± 0.5	13.0± 0.4	1.8± 0.3	4.3± 0.2	0.0± 0.3	1.0± 0.1
5.0	11.2± 0.5	11.4± 0.2	3.6± 0.3	2.9± 0.2	0.7± 0.3	0.9± 0.1
8.0	9.6± 0.5	10.2± 0.2	3.0± 0.3	3.4± 0.1	0.7± 0.3	0.8± 0.1
11.0	8.9± 0.5	9.1± 0.3	2.8± 0.3	2.9± 0.2	0.5± 0.3	0.7± 0.1

Table 5: The percentage of the Čerenkov radiation produced at greater than a certain angle with respect to the electron's initial direction. The 'EGS4' column is with ESTEPE set at 3 % .

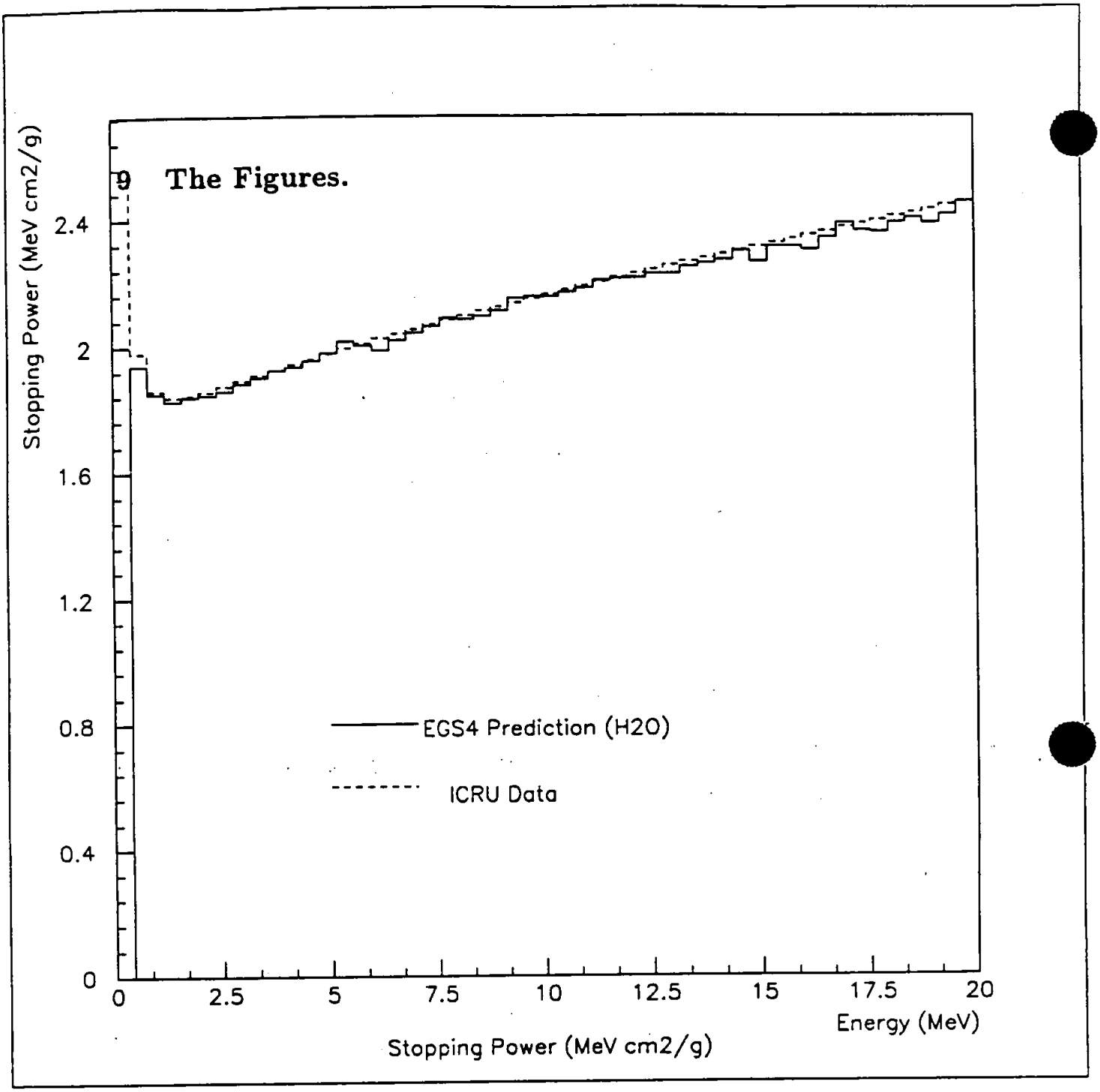

Figure 1: The stopping power of H_2O plotted with the data from the ICRU data.

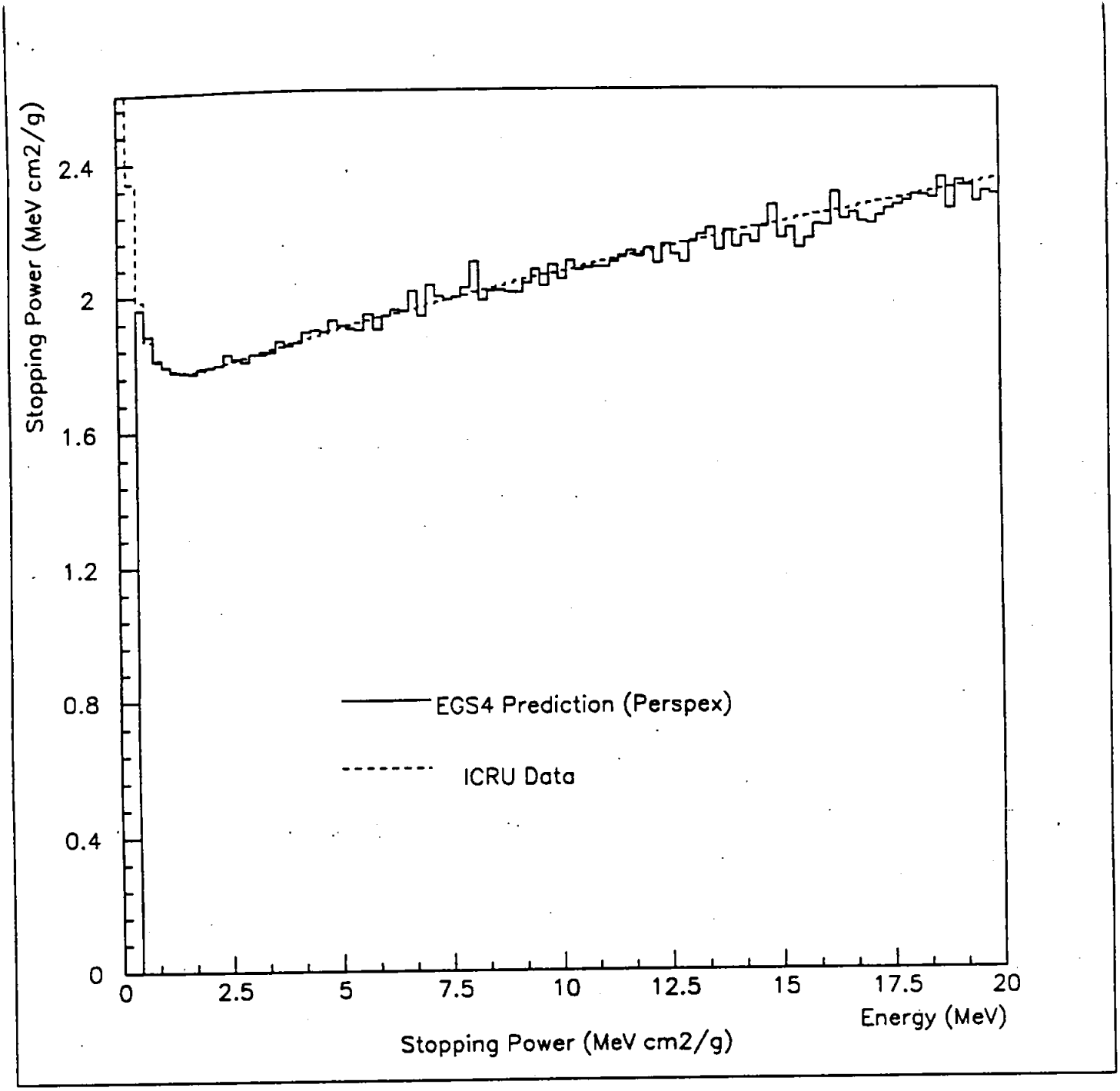

Figure 2: The stopping power of perspex plotted with the data from the ICRU data.

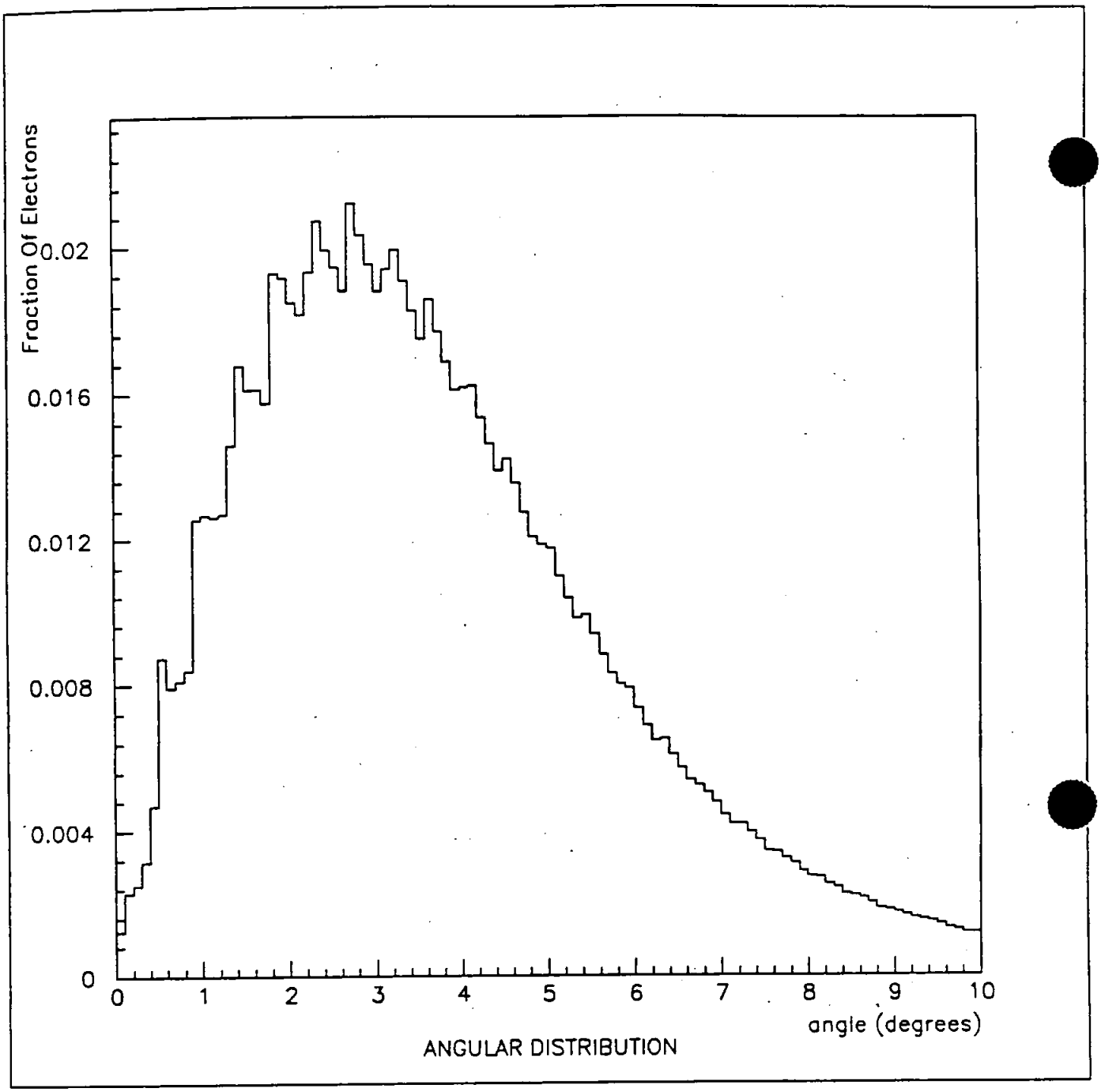

Figure 3: The angular distribution of 15.7 MeV electrons on a thin gold foil, showing 'plateau' structure.

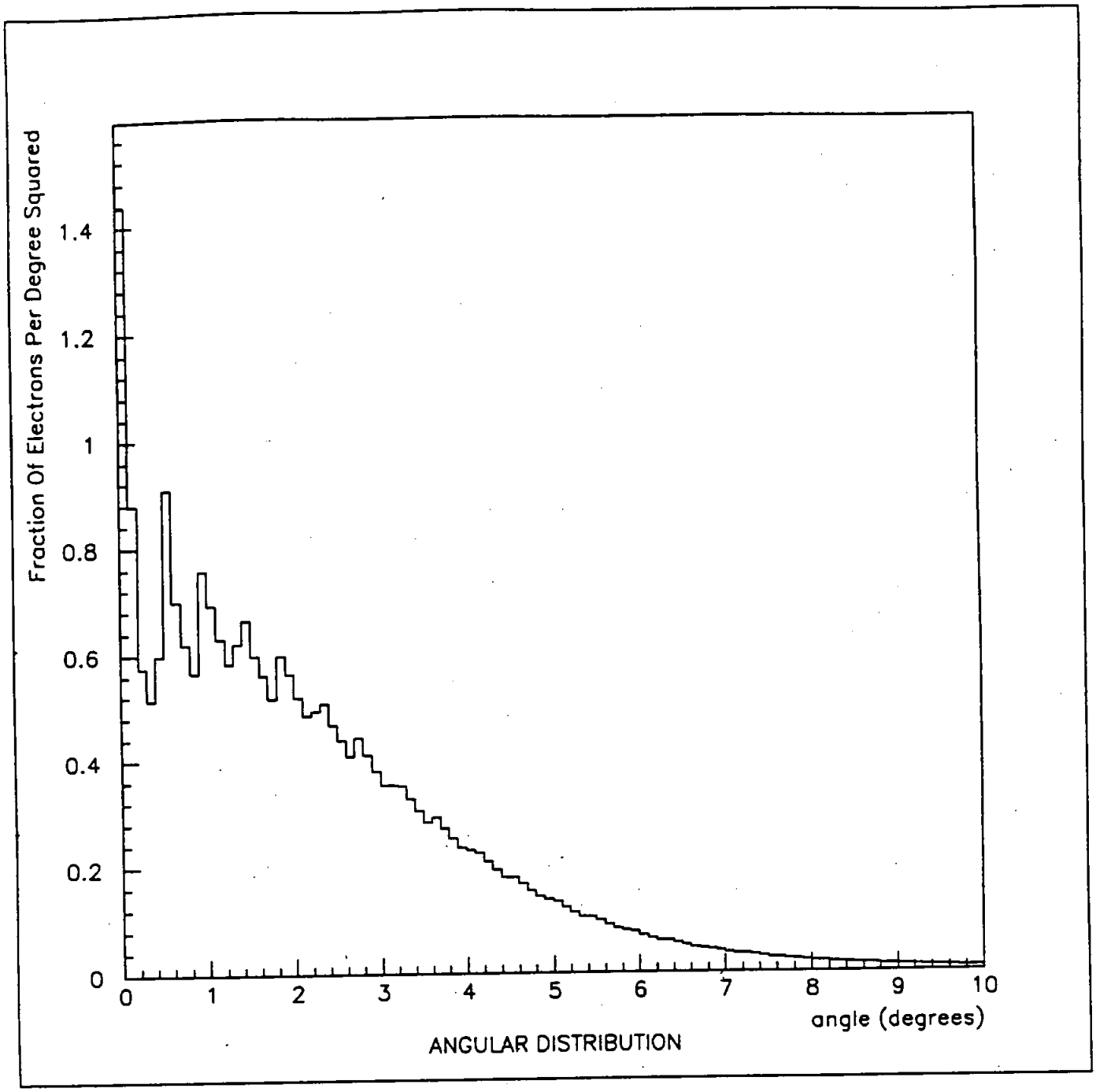

Figure 4: The angular distribution of 15.7 MeV electrons on a thin gold foil, showing 'plateau' structure, divided by $\sin\theta$.

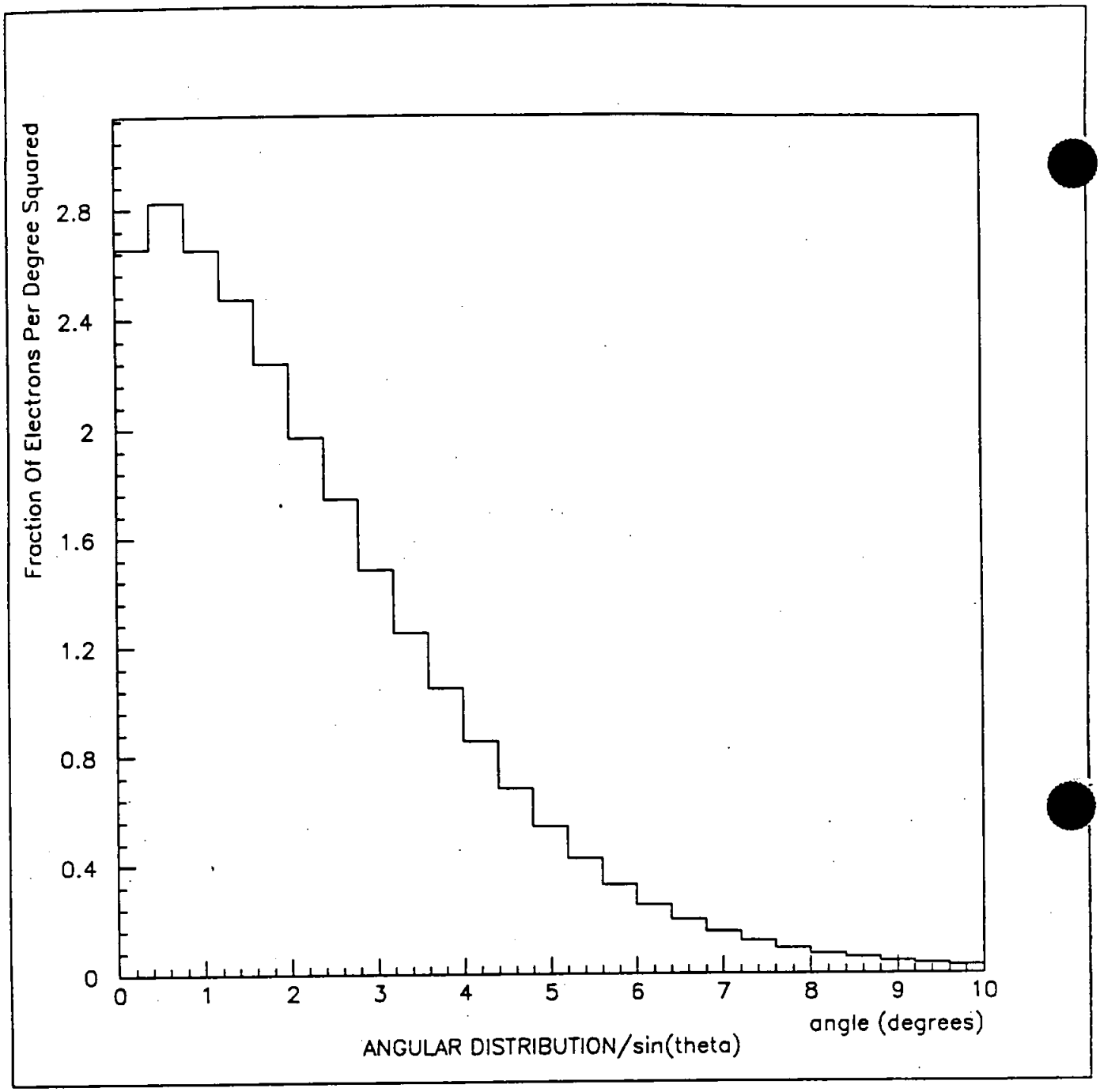

Figure 5: The angular distribution of 15.7 MeV electrons on a thin gold foil, with larger bin widths, divided by $\sin\theta$. Note that most of the peaked structure is washed out.

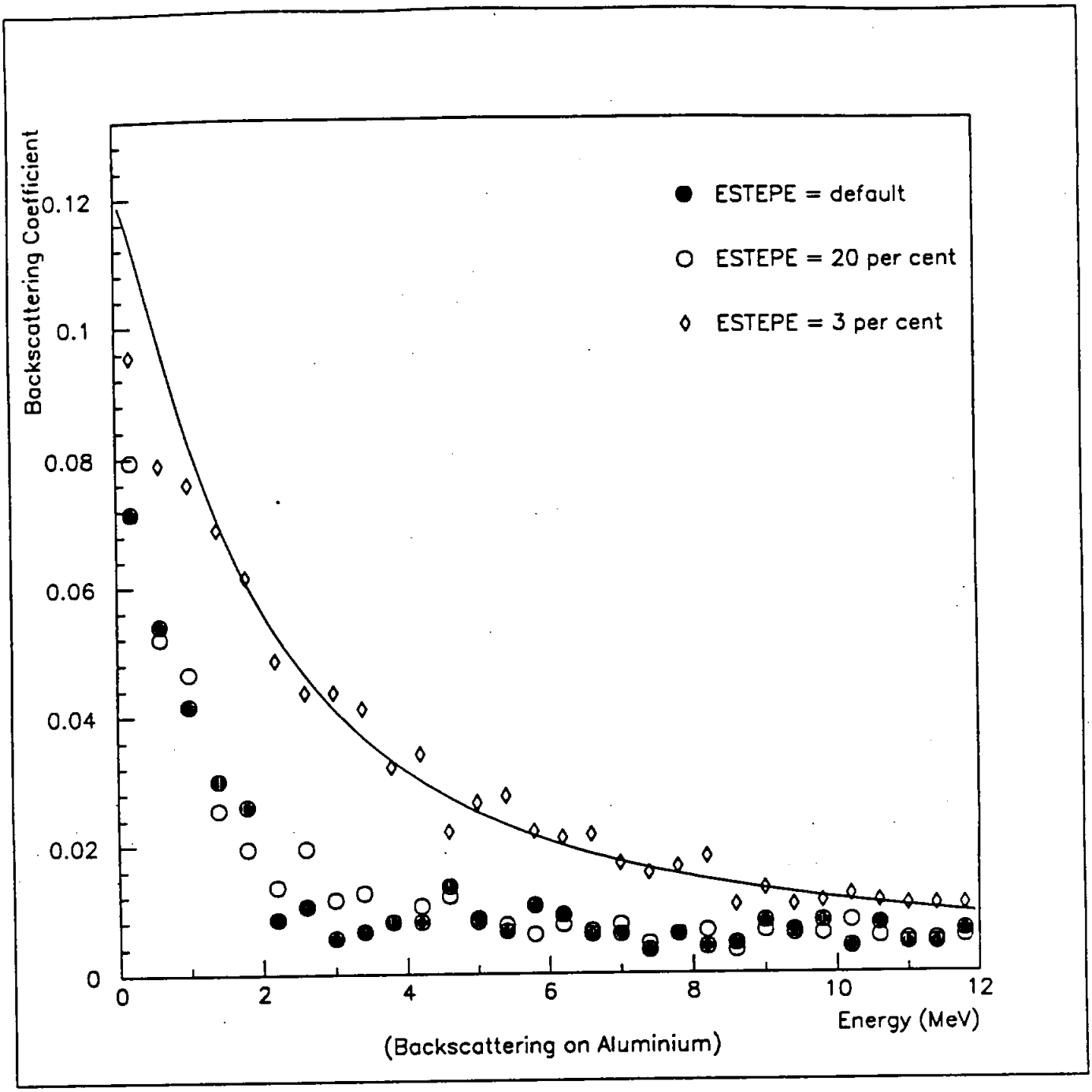

Figure 6: A comparison of the experimental data and EGS4 predictions for aluminium.

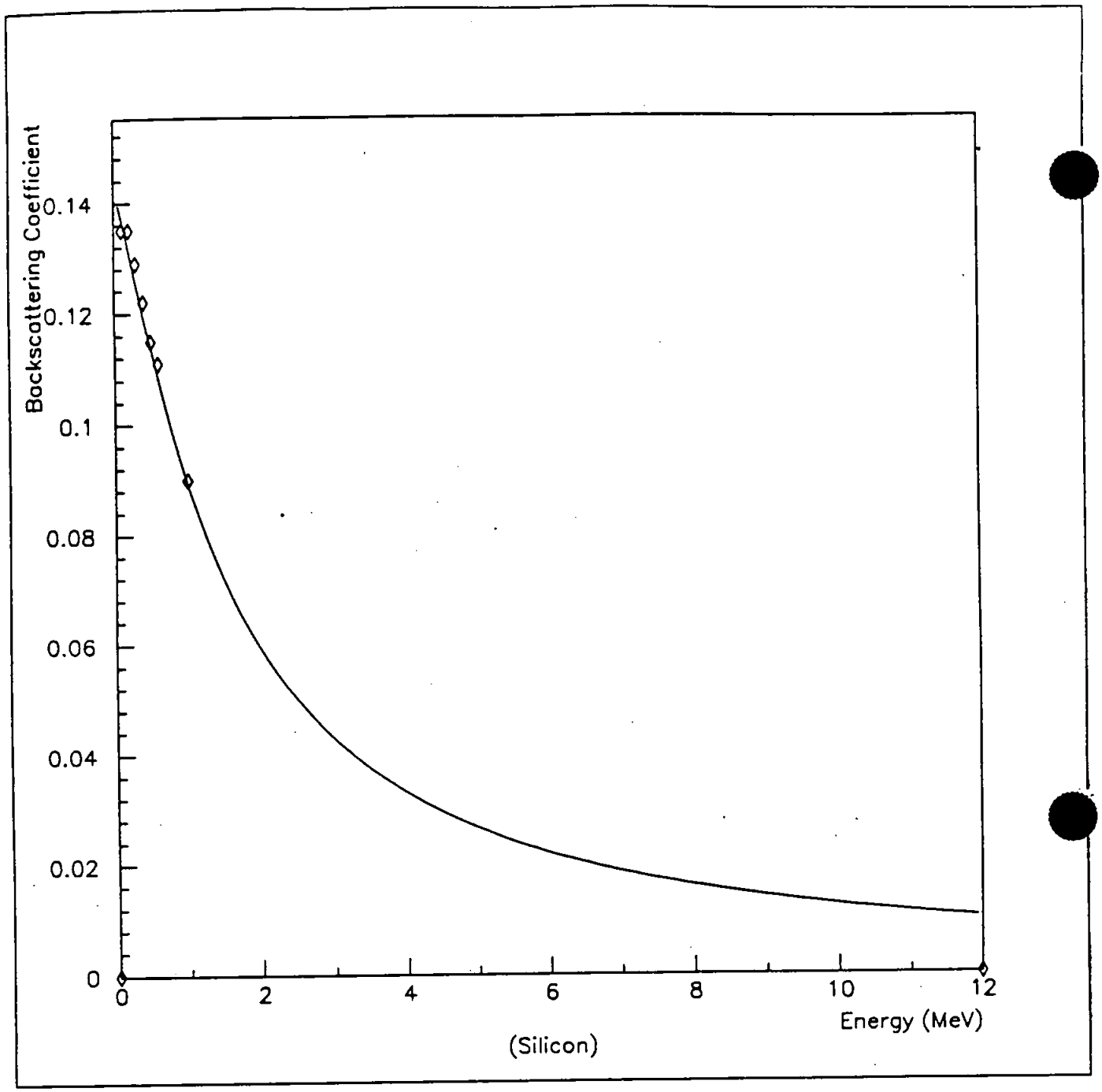

Figure 7: A comparison of available data and the predictions made by Tabata et al for silicon.

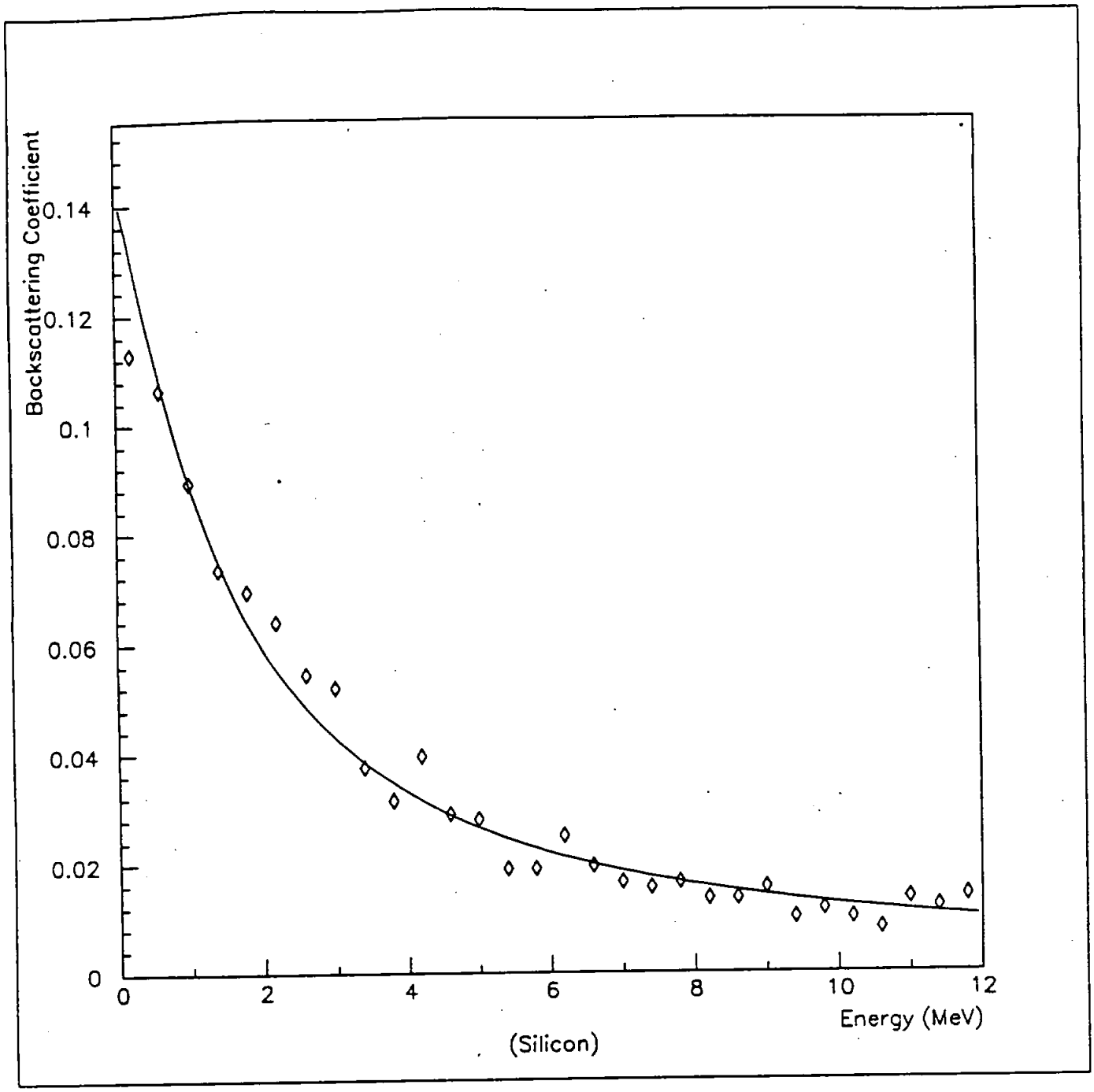

Figure 8: A comparison of the experimental data and EGS4 predictions for silicon.

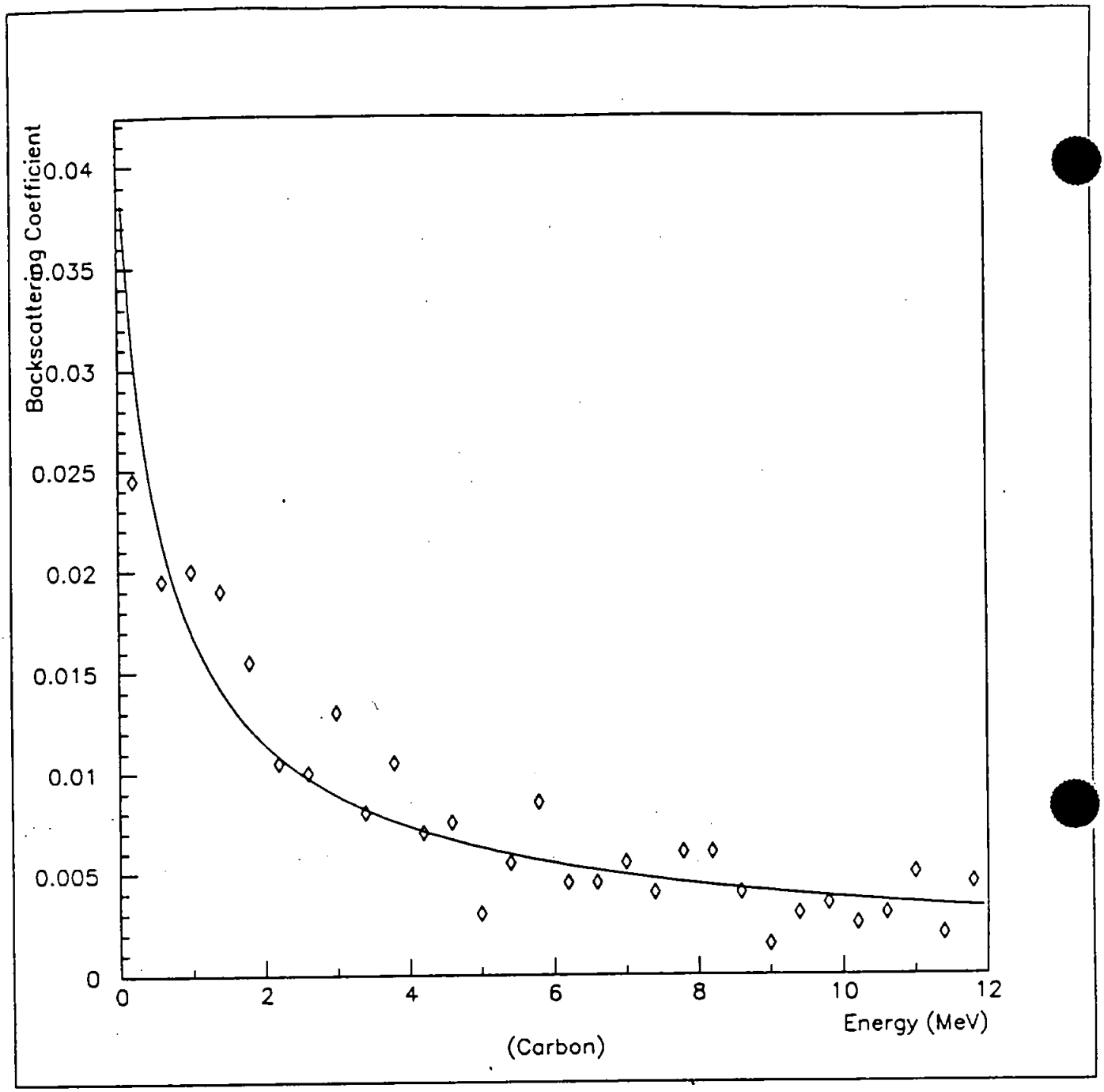

Figure 9: A comparison of the experimental data and EGS4 predictions for carbon.

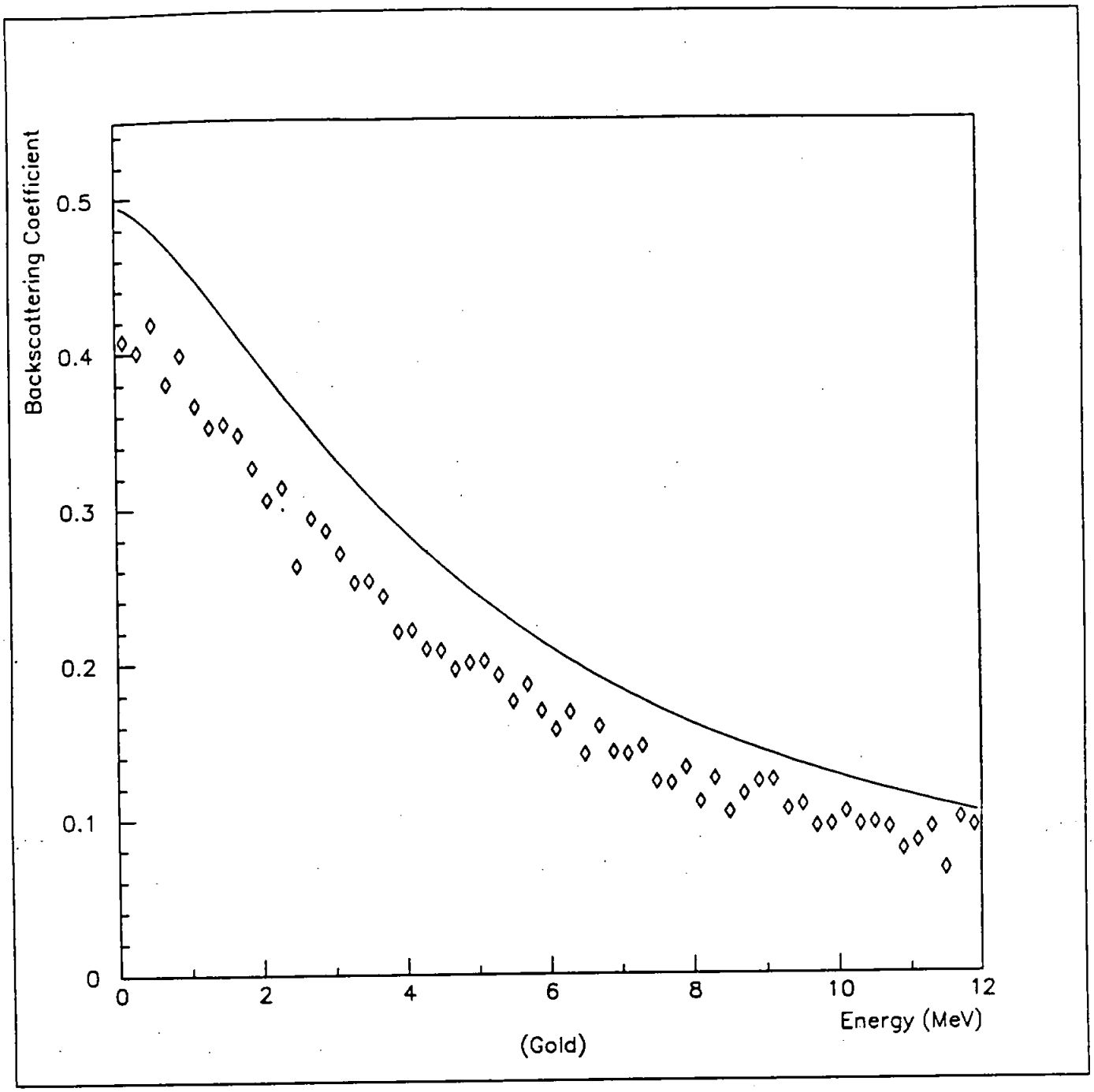

Figure 10: A comparison of the EGS4 predictions and Tabata's data for the backscattering coefficient from gold. ESTEPE = 3%.

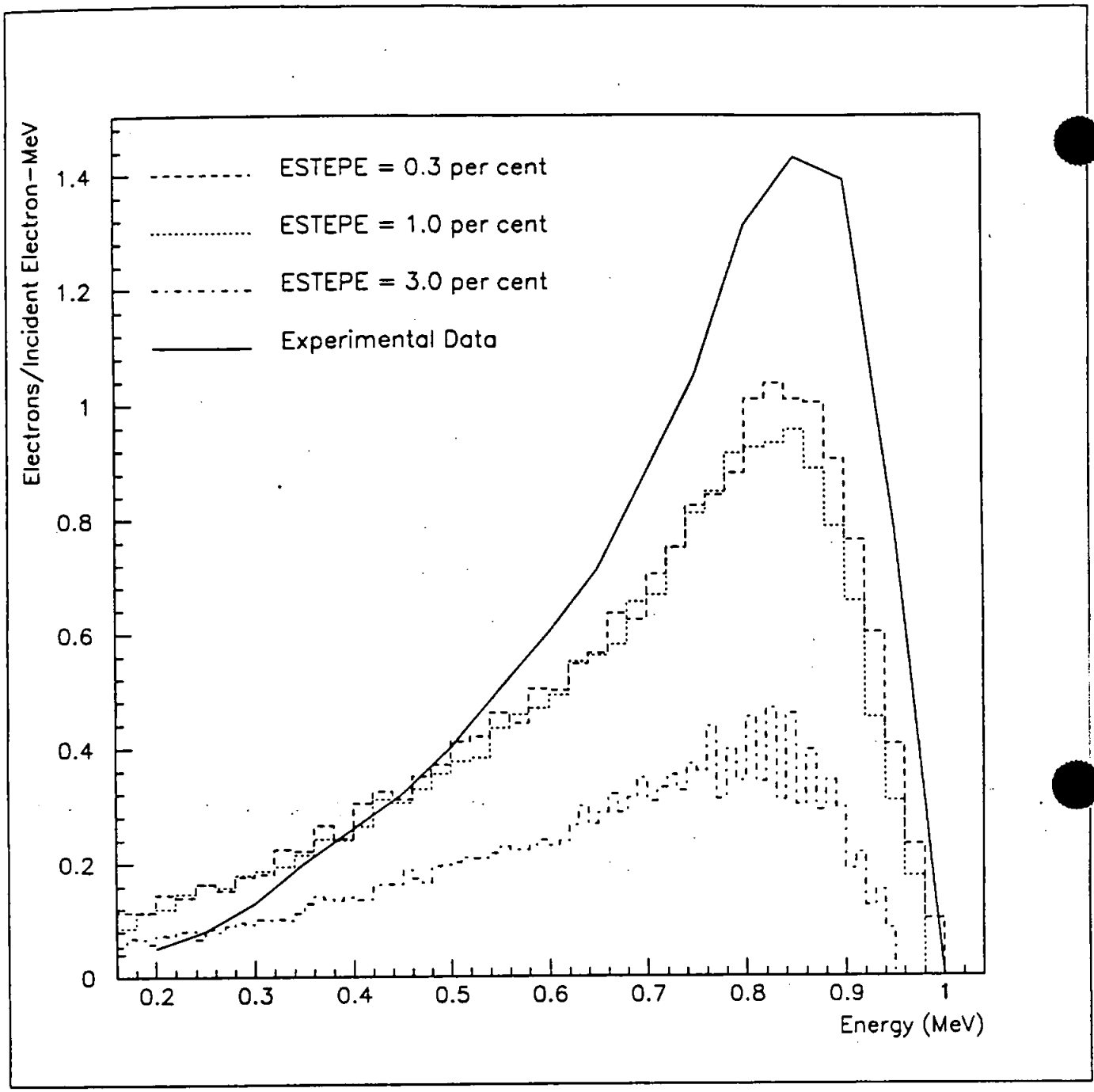

Figure 11: A comparison of the EGS4 predictions for the kinetic energy spectrum of 1 MeV electrons backscattered from gold.

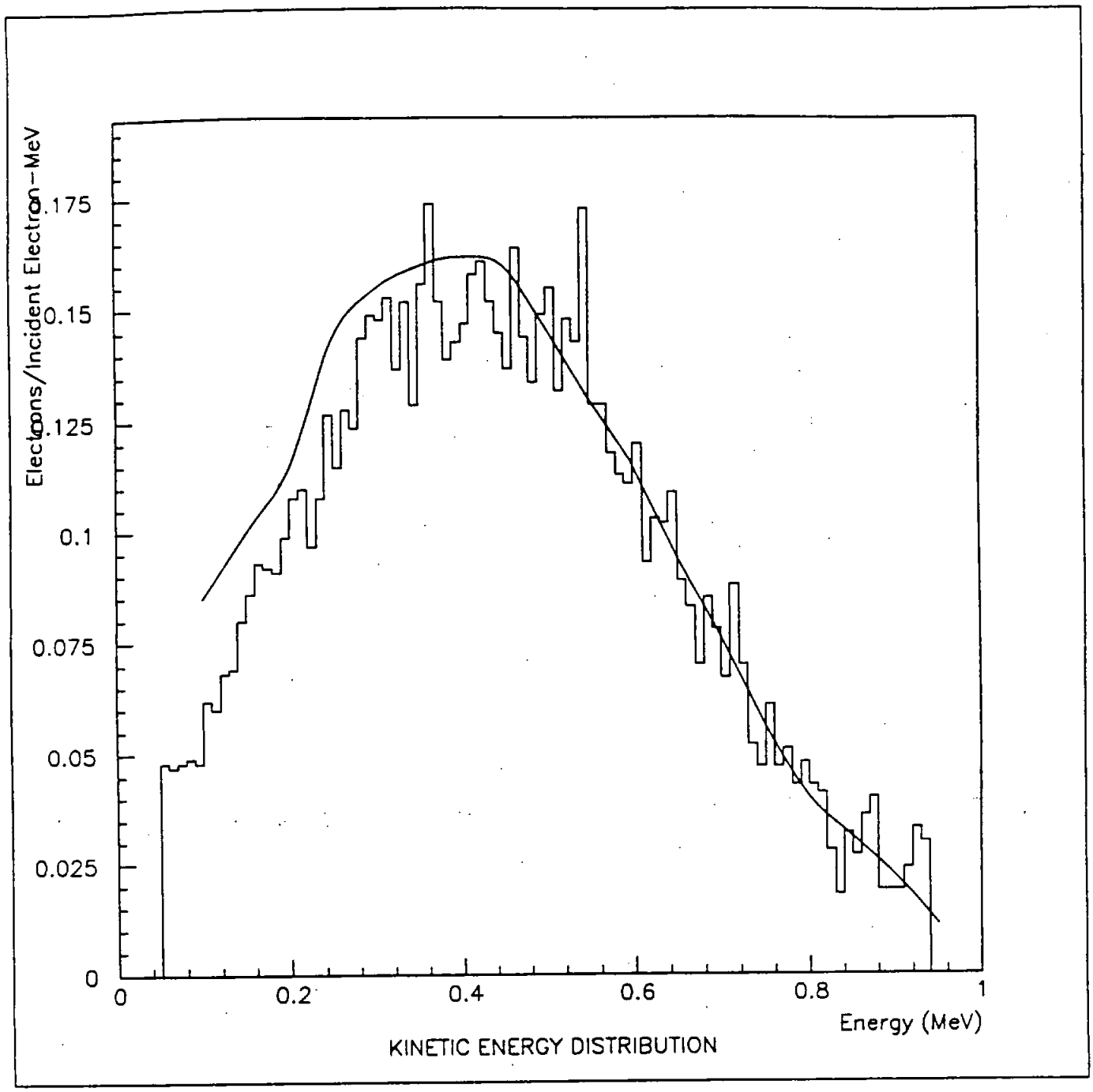

Figure 12: A comparison of the experimental data and EGS4 predictions for 1 MeV electrons backscattered from aluminium.

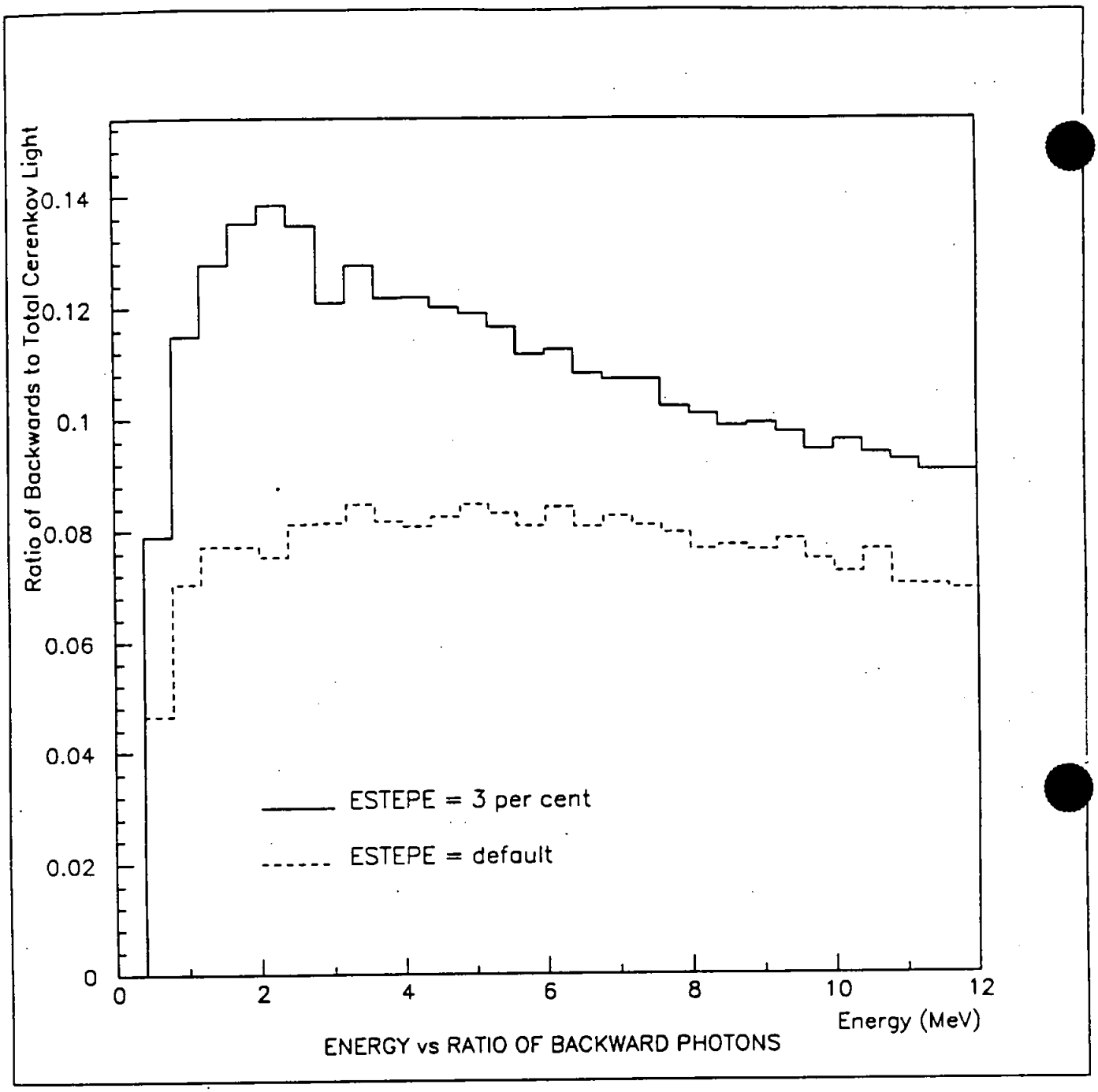

Figure 13: The ratio of backward to forward Čerenkov radiation production for ESTEPE at 3% and at the default.